Benvenuti, T.; García Gabaldón, M.; Ortega Navarro, EM.; Rodrigues, M.; Bernardes, A.; Pérez-Herranz, V.; Zoppas-Ferreira, J. (2017). Influence of the co-ions on the transport of sulfate through anion exchange membranes. Journal of Membrane Science. 542:320-328. doi:10.1016/j.memsci.2017.08.021

Influence of the co-ions on the transport of sulfate through anion exchange membranes

T. Benvenuti [a,1]; M. García-Gabaldón [b]; E. M. Ortega [b]; M.A.S. Rodrigues[c]; A. M. Bernardes [a], V. Pérez-Herranz[b]; J. Zoppas-Ferreira [a]

[a] *LACOR, PPGE3M, Universidade Federal do Rio Grande do Sul, Av. Bento Gonçalves, 9500, Setor 4, Prédio 43426, Campus do Vale, 91509-900 Porto Alegre, RS, Brazil*

[b] *IEC Group, Departament d'Enginyeria Quimica i Nuclear, Universitat Politècnica de València, Camí de Vera s/n, 46022, València, P.O. Box 22012, E-46071, Spain.*

[c] *Instituto de Ciências Exatas e Tecnológicas, Universidade FEEVALE, RS 239, 2755, B.Vila Nova, CEP: 93.352-900 Novo Hamburgo, RS, Brazi.l*

Abstract

The increasing demand for clean industrial processes has intensified the use of electrodialysis (ED) in the treatment of metal containing effluents from plating processes. Nickel rinsewater is a multicomponent solution that can be treated by ED in order to recover chemicals and reuse water. The investigation of the different phenomena involved in the transport of anions through anion-exchange membranes in this wastewater has been performed in different synthetic solutions by chronopotentiometry. Parameters like the limiting current density (i_{lim}), the plateau length (ΔU_m), the resistance of the ohmic region (R_{ohm}) and the resistance of the overlimiting region (R_3) were also determined. Even though an anion exchange membrane (AEM), the limiting current density was affected by the proton leakage phenomena, indicated that the proton H^+ has a greater effect than the other co-ions (Ni^{2+}, Mg^{2+} and Na^+). Ohmic resistances were reduced and plateau lengths were increased in the presence of protons. For salts solutions (without acid) the highest diffusion coefficients and lowest co-ion hydrated radii gave the highest plateau lengths and i_{lim}, but the lowest R_{ohm}.

Keywords: Anion-exchange membrane. Sulfate anion transport. Proton leakage. Co-ion effect

[1] Corresponding author: benvenuti.tatiane@gmail.com

1. Introduction

Nickel plating rinsewater can be treated by electrodialysis (ED) in order to recover chemicals and reuse water. Previous works [1] indicated that different chemical species may exist in the nickel electroplating wastewater, depending on the pH, including Ni-anion inorganic complexes such as $[Ni(SO_4)_2]^{2-}$. This negatively charged compound may also affect the nickel transport, enabling the passage of the metal through the anionic membranes during electrodialysis [2–4]. Nickel transported through the anionic membranes can reach the electrodes solution and can be reduced and deposited on the cathode or oxidized on the anode. Industrial applications of ED that gave rise to this study indicated that nickel deposited as metal or oxide on the electrodes can reduce the electrodes useful area and affect ED operational parameters as the electric current density. The increase in the current density can intensify the electrodes reactions, causing changes in the pH. Alkaline pH causes the metal precipitation as hydroxide on the membranes, reducing the treatment efficiency, by the variations in the useful membrane area and hampering the ions transport.

In the literature, there was no additional information about the transport of Ni-anion inorganic complexes through anion-exchange membranes and their related behavior during ED treatment.

Nickel bright plating processes are performed with acid baths and organic additives that also compose the rinsewater. In order to avoid the nickel precipitation and scaling on the membranes, a pH adjustment can also be performed during the treatment by electrodialysis. The addition of acid, normally H_2SO_4 changes the electric conductivity, the anion concentration and consequently operational parameters for ED treatment. Studies about ED and electro-electrodialysis (EED) showed the proton leakage through anion-exchange membranes and reported the mechanisms involved in this transport phenomena [5–10]. Proton leakage is a problem when the goal of the treatment is the recovery of acid [5] affecting the transport of other ions and the operational parameters.

Analytical techniques, such as chronopotentiometry, have been applied in order to investigate the ion transport through ion-exchange membranes [3,7,11]. Chronopotentiometry is a dynamic electrochemical technique that is useful to identify

different phenomena taking place in interfacial processes. In the case of the study of monopolar ion-exchange membranes (IEMs) used in electrodialysis, chronopotentiometry has been applied to evaluate the transport properties of different ions through the IEMs. These measurements give important information about the heterogeneity, electric conductivity, permselectivity and transport number. Furthermore, this technique represents an indirect measure of changes in the solution composition on the membrane-solution interface, allowing the study of the effects caused by concentration polarization (water splitting, gravitational convection and electroconvection), fouling and scaling. Chronopotentiometry is also a useful tool for the study of the behavior of bipolar membranes [4,12,13].

Associated to the chronopotentiometric measures, the current-voltage curve (i-U_m curve) corresponding to the membrane system is a frequently used method to characterize the transport properties of ion-exchange membranes. The typical profile of these curves is associated with the concentration polarization phenomenon, and presents three regions: a quasi-linear region at low concentration polarization, a horizontal plateau corresponding to the limiting current density, i_{lim}, and an overlimiting region, which could indicate several mechanisms involving water splitting, electroconvection, gravitational convection and changes in the limiting diffusion layer [14].

The aim of the present work is to investigate the ion transport through an anion-exchange membrane in synthetic nickel rinse plating baths with sulfate as anionic component using chronopotentiometry. The novelty of this study is related to the gap in the literature about the transport of anions and metal-complexes through anion exchange membranes in solutions containing metals. Since when solutions with metals are treated by ED, the investigations about ions transport are focused in cations exchange membranes. In addition, the evaluation of the effect of counter and co-ion concentration and characteristics were also considered. Solutions of sulfuric acid, sodium sulfate, magnesium sulfate and bicomponent solutions have also been tested in order to evaluate the effect of pH, counter and co-ion concentrations. From the i-U_m curves, important transport properties like the resistance of the ohmic region and the plateau length were obtained. Additionally, the speciation diagrams as a function of the pH were evaluated for all solutions in order to explain the transport phenomena.

2. Materials and methods

2.1. Membranes

The membranes used in the experiments were produced by Resindion S.r.l., Italy. The anion-exchange membrane (AEM) evaluated is an IONAC MA-3475, a heterogeneous membrane made of polyvinylidene fluoride (PVDF) containing quaternary amine as a functional group. The cation exchange membrane (CEM), IONAC MC-3470, is also heterogeneous and made of PVDF with sulfonic acid as a functional group. The technical characteristics of both membranes are presented in Table 1.

Table 1 – Technical characteristics of the CEM and the AEM [15].

Parameter	**Unit**	**MC-3470**	**MA-3475**
Electrical Resistance			
0,1N NaCl	$ohm.cm^{-2}$	15	24
1,0N NaCl		6	8
Permiselectivity (0,5N NaCl/1,0N NaCl)	%	96	75
Thickness	mm	0.4	0.4
Ion Exchange Capacity (dry basis)	meq/g	1,25	1,00
Water Permeability (in 0,35 $kg.cm^{-2}$)	$mL.h^{-1}.dm^{-2}$	<3.2	<3.2
Burst strenght	$kg.cm^{-2}$	≥ 14	≥ 14

2.2. Solutions and Reagents

All reagents used in the experiments were of analytical grade. Synthetic solutions based on the composition of the nickel rinse plating baths were prepared with $NiSO_4.6H_2O$. In order to compare the co-ion effect, Na_2SO_4, $MgSO_4$ and H_2SO_4 solutions were also used. Sodium is a very common ion in nickel plating bath since is present in the formulation of organic additives (sodium saccharin, alkyl sodium sulfonate). On the other hand, magnesium was selected as a bivalent cation whose behavior could be comparable to Ni^{2+}. The pH was adjusted by adding H_2SO_4 in sodium and nickel solutions. As related in previous work [1], H_2SO_4 could be added to the

wastewater during the ED treatment in order to avoid the nickel precipitation. The solution concentration varied from 1×10^{-2} M to 2×10^{-2} M, pH and conductivity were measured before and after the chronopotentiometric analysis. Information about the studied solutions is presented in Table 2.

Table 2 – Characteristics of the sulfate solutions.

Solution	**C_0 (M)**	**Initial $[SO_4^{2-}]$ (M)**	**pH**	**Electric conductivity ($\mu S.cm^{-1}$)**	**Ionic strength (M)**
1. $NiSO_4.6H_2O$	1.05×10^{-2}	1.05×10^{-2}	4.4-4.1	1444	4.2×10^{-2}
2. $NiSO_4.6H_2O$ + H_2SO_4	1.05×10^{-2} + 4.4×10^{-3}	1.49×10^{-2}	2-2.2	4130	5.52×10^{-2}
3. H_2SO_4	1.05×10^{-2}	1.05×10^{-2}	1.85	6180	3.15×10^{-2}
4. Na_2SO_4	1.05×10^{-2}	1.05×10^{-2}	8.2-7.9	1694	3.15×10^{-2}
5. Na_2SO_4 + H_2SO_4	1.05×10^{-2} + 1.1×10^{-3}	1.16×10^{-2}	1.9-2.0	3500	3.28×10^{-2}
6. $MgSO_4$	1.94×10^{-2}	1.94×10^{-2}	6.7	1740	7.76×10^{-2}
7. Na_2SO_4 + $NiSO_4$	1.05×10^{-2} + 1.1×10^{-3}	1.16×10^{-2}	7.2-7.3	1709	3.59×10^{-2}

2.3. Experimental setup

The experimental setup used in the chronopotentiometric experiments is shown in Figure 1 and is composed of an acrylic three compartment cell of 220 mL each, separated by the AEM and the CEM. The membrane effective area was 16 cm². The cation-exchange membrane is used to separate the cathodic compartment from the central compartment and minimize the contribution of the OH^- generated at the cathode on the anion-exchange membrane measurements. Prior to each chronopotentiometric experiment, the membranes were equilibrated during 24 h, under stirring, immersed in the same solutions as those used in the experiments. After this period, the fixed charges are supposed to be in equilibrium with the counter-ions present in the solution and membranes are ready to be used.

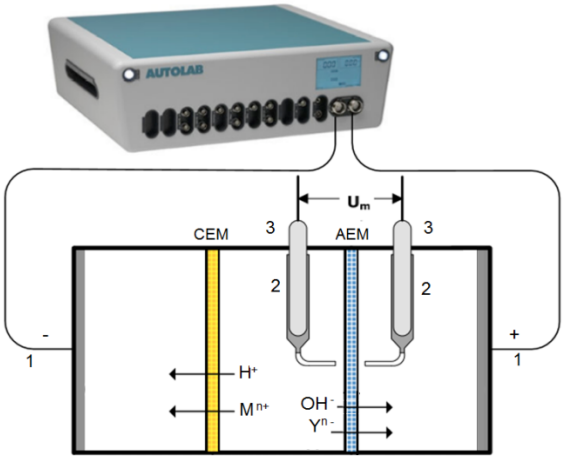

Figure 1. Experimental setup used during the electrochemical measurements. (1) graphite electrodes, (2) Luggin capillaries, (3) two reference electrodes Ag/AgCl, AEM and CEM- ion exchange membranes (A-anion, C-cation).

Chronopotentiometric experiments were performed based on previous researches [3,4,13,16–18]. Tests were performed in duplicate, at room temperature and with no stirring. A constant current was imposed between the graphite electrodes by means of a potentiostat/galvanostat (Autolab, PGSTAT302). Two Ag/AgCl reference electrodes immersed in Luggin capillaries were installed each one in each side of the AEM to measure the voltage drop (U_m) across the membrane. The imposed current promotes the cations motion from central to the cathodic compartment across the CEM, and the anions from the central to the anodic compartment through the AEM. Different current pulses were imposed with pulse duration of 120 s. When the current pulse is interrupted (I=0 mA), the relaxation process of the system is allowed during 120 additional seconds, before a new incremented pulse is applied. The time of 120 s for current pulse and relaxation was based on previous works [16]. The response of the measured membrane voltage drop between the Lugging capillaries, U_m (V), was registered during the tests by the NOVA® 10.1 Autolab software.

The i-U_m curves were obtained from the steady-state values of the voltage drop through the membrane obtained for a given applied current pulse in the chronopotentiometric experiments. In order to investigate the ion transport through the anion-exchange membrane IONAC MA 3475, the solutions are assessed according to Figure 2.

Effect of pH and sulfate concentration in nickel effluents: $NiSO_4$, $NiSO_4$+H_2SO_4 and H_2SO_4	Effect of co-ion properties in mono and bicomponent solutions $MgSO_4$, Na_2SO_4, Na_2SO_4+H_2SO_4, $NiSO_4$ and Na_2SO_4 + $NiSO_4$

Figure 2. Block-diagram presenting the solutions assessment.

3. RESULTS AND DISCUSSIONS

3.1. Effect of pH and sulfate concentration

On the basis of the previous evaluation of chemical speciation diagrams, the solutions under study intent to show the behavior of sulfate transport through anion-exchange membranes in synthetic solutions and the possible effects of anionic nickel complexes.

In order to investigate the co-ion effect on the anion transport, nickel sulfate solution (without H_2SO_4) and a sulfuric acid solution with the same initial concentration of SO_4^{2-} ($1.05 \cdot 10^{-2}$ M) were compared in Figure 3.

a)

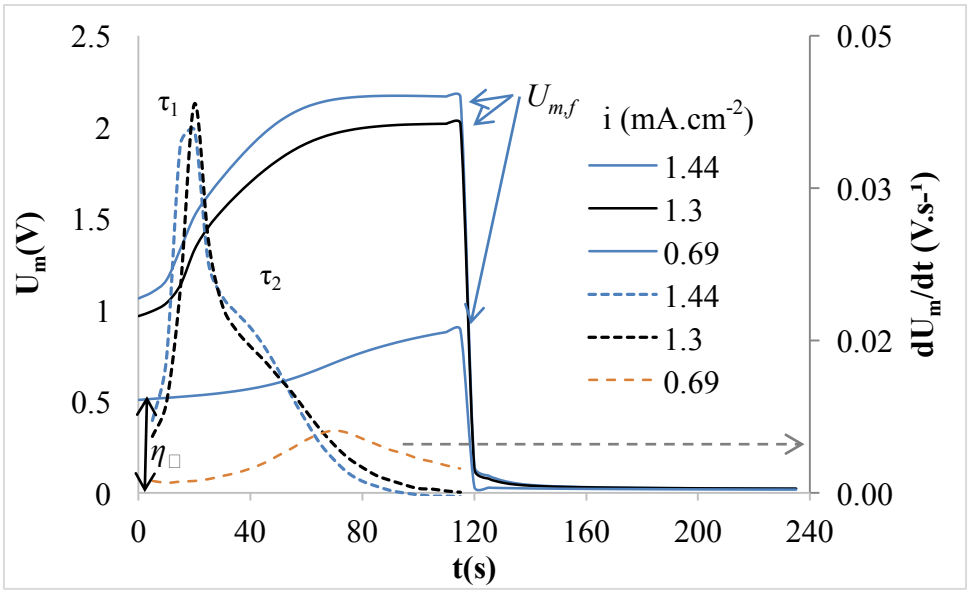

b)

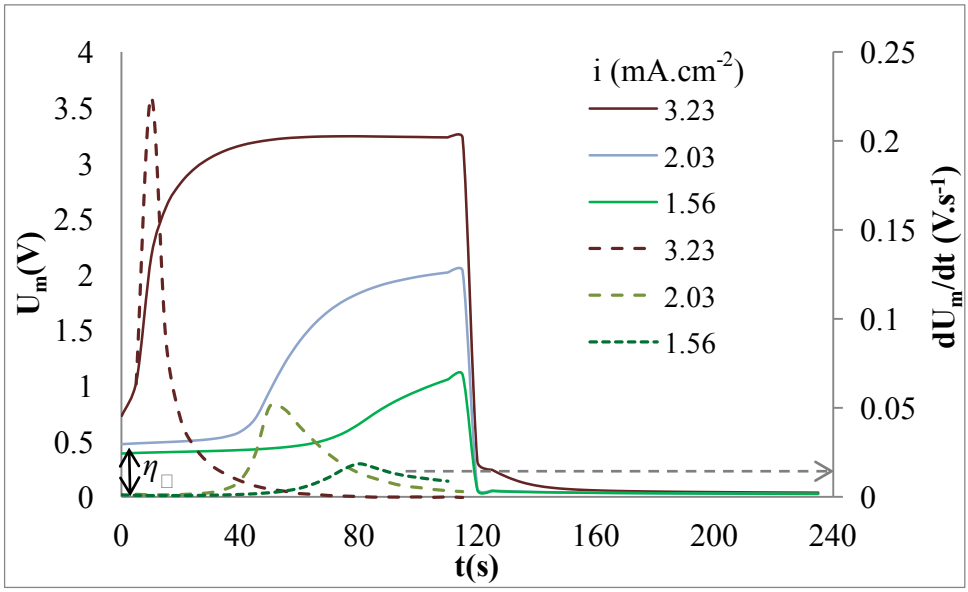

c)

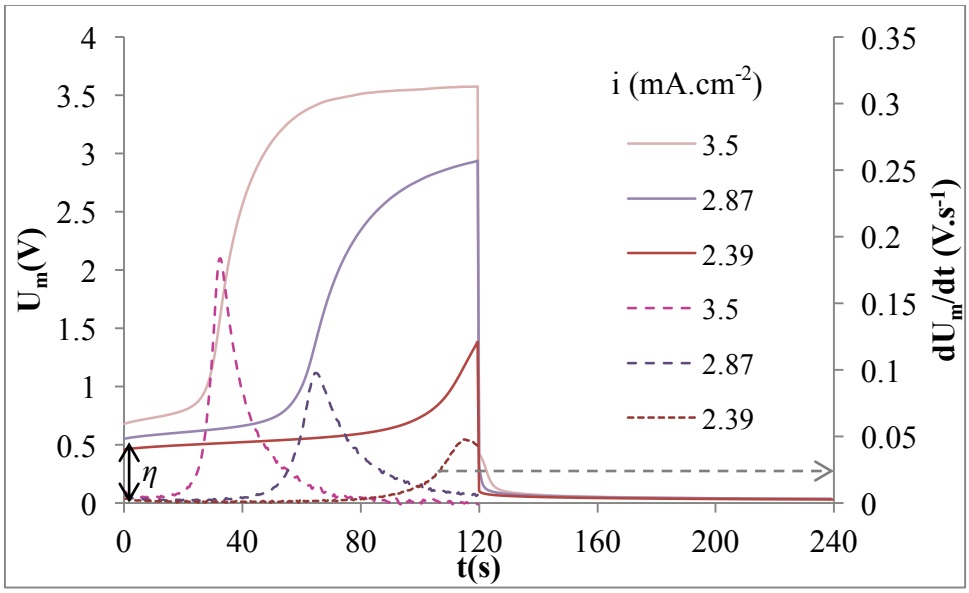

Figure 3. Chronopotentiograms obtained for the anion exchange membrane Ionac MA 3475 in (a) $NiSO_4$ 1.05□10^{-2} M; (b) $NiSO_4$ 1.05□10^{-2} M + H_2SO_4 4.4□10^{-3} M and (c) H_2SO_4 1.05□10^{-2} M solutions. (Solid line: U_m (V); dashed line: dU_m/dt ($V.s^{-1}$)).

At the beginning of the current pulse an immediate increase of U_m is observed in the curves, which is related to the ohmic overvoltage (η_Ω) of the membrane. The η_Ω for both systems shows a similar value, around 0.4-0.5 V, when the first transition time was detected. The same behavior can be verified for the last registered potential, $U_{m,f}$ (0.89-1.36 V). These values are indicated in Table 3. For the less conductive solution, $U_{m,f}$ is higher and the transition time shorter, for the same value of applied current, indicating an important effect related to the presence of H_2SO_4. Due to the high electrical

conductivity and mobility of the proton, the acid increases the solution conductivity, whose influence seems to be more pronounced than the total solution concentration.

Table 3 - Values of ohmic overvoltage (η_{Ω}), first transition time (τ_1) and respective electric current density (i), final steady-state potential ($U_{m,f}$) and electric conductivity of nickel and sulfuric acid solutions.

Solution	τ_1 (s)	i (mA.cm^{-2})	η_{Ω} (V)	$U_{m,f}$ (V)	Electric conductivity (μS.cm^{-1})
1. $NiSO_4.6H_2O$	75	0.69	0.516	0.89	1444
2. $NiSO_4.6H_2O$ + H_2SO_4	80	1.56	0.39	1.1	4130
3. H_2SO_4	115.5	2.39	0.47	1.36	6180

The chronopotentiometric curves presented in Figure 3 correspond to the typical chronopotentiograms for monopolar membranes [16]. The curves are smooth and the inflection regions are diffuse what is characteristic for heterogeneous membrane [19]. All presented curves are above the limiting current value and this fact explains the appearance of the transition time (τ), which is defined as the time taken for the ion depletion at the membrane surface when a constant current is applied. Based on the corresponding chronopotentiometric curve, the transition time can be determined as the maximum of the derivative of the voltage drop, U_m, with time. When making a comparison between the curves of the sulfate solutions, some differences can be found. The first transition time observed for each solution was 75 s, 80 s and 115.5 s to $NiSO_4$, $NiSO_4$+H_2SO_4 and H_2SO_4 solutions, respectively.

Additionally, the solution composition caused differences in the curve shape, giving two transition times for $NiSO_4$ (Figure 3 a) when the applied current is further increased. The second inflexion point (transition time τ_2= 50 s, i=1.3 mA.cm^{-2}) corresponds to the depletion/transport of other anionic species present in the electrolyte [3,4]. In this sense, the species in equilibrium for each solution were obtained by speciation diagrams, generated by the HydraMedusa® software, and are indicated in Table 4.

For $NiSO_4$ solution, in the initial pH around 4.4, the predominant anionic specie is SO_4^{2-}, followed by HSO_4^- ion, and additionally, a nickel-sulfate complex $[Ni(SO_4)_2]^{2-}$, in lower concentration, as presented in the Table 4. In view of the higher charge and smaller size of SO_4^{2-} in comparison with HSO_4^- ions, the first increase in *Um* observed for low values of current density (Figure 3) may be attributed to the depletion of SO_4^{2-} ions in the diluted diffusion boundary layer. When SO_4^{2-} ions are depleted from the solution/membrane interface the main charge carrier changes from SO_4^{2-} to HSO_4^- ions. The concentration of the nickel-sulfate complex $[Ni(SO_4)_2]^{2-}$ is considerably lower than HSO_4^-, therefore, the depletion of HSO_4^- ions from the diffusion boundary layer is probably responsible for the second transition time appearing in the highest current densities presented in Figure 3.

When sulfuric acid was added to the nickel sulfate solution (Figure 3 (b)), the first transition time and the corresponding electric current are higher than the values observed for pure $NiSO_4$. These changes indicate that in more concentrated solutions, higher current densities are necessary to transport charges through the membrane until reaching the ion depletion in the membrane-solution interface [20]. In this acidified solution, the second transition time was not observed. As observed in Table 4, the concentration of the HSO_4^- ion is close to SO_4^{2-} and their transition times can be overlapped, since the increasing in U_m becomes bigger and steeper with the increase of the applied current density. The absence of the second transition time is similar to previous results obtained for cation-exchange membranes in $Cr_2(SO_4)_3$ solutions [3], where in the case of low concentrations, two inflection points were verified, whereas only one was detected in higher concentration values.

Table 4 - Concentration (mol/L) of the species present in equilibrium as a function of the initial solution concentration and pH.

Solution	$NiSO_4.6H_2O$	$NiSO_4.6H_2O+H_2SO_4$	H_2SO_4
Concentration	$1.05\square10^{-2}$ M	$1.05\square10^{-2}$ M+$4.4\square10^{-3}$ M	$1.05\square10^{-2}$ M
pH	4.4	2.1	1.85
$[NiSO_4]_{(aq)}$	$5.01\square10^{-3}$	$5.01\square10^{-3}$	-
$[H_2SO_4]_{(aq)}$	-	$3.16\square10^{-7}$	$8.71\square10^{-7}$
$[H^+]$	$8.71\square10^{-5}$	$7.94\square10^{-3}$	$1.41\square10^{-2}$
$[Ni^{2+}]$	$5.13\square10^{-3}$	$5.62\square10^{-3}$	-
$[NiOH^+]$	$2.14\square10^{-8}$	-	-
$[OH^-]$	-	-	-
$[SO_4^{2-}]$	$5.13\square10^{-3}$	$5.13\square10^{-3}$	$4.57\square10^{-3}$
$[HSO_4^-]$	$4.27\square10^{-5}$	$4.68\square10^{-3}$	$5.62\square10^{-3}$
$[Ni(SO_4)_2^{2-}]$	$1.45\square10^{-6}$	$1.53\square10^{-6}$	-

The H_2SO_4 solution presented chronopotentiometric curves similar to the nickel acidified solution. According to Figure 3 and Table 3, the transition time and the current density whereby the first transition time was detected are higher for H_2SO_4 solution than in the previous one. This effect seems to be more related to the electric conductivity than to the initial sulfate ions concentration [21]. Once the initial concentration for $NiSO_4$ and H_2SO_4 was the same, $1.05\square10^{-2}$ M, the limiting current density suffers the influence of additional factors as the diffusivity, mobility and conductivity of the ionic species in solution. For H_2SO_4 and also for the mixed Ni-acid solution, the presence of protons affects the properties of the studied solutions in a big way. Comparing the data presented in Table 4, the presence of acid and the low pH confers to the solutions a very close concentration of the main sulfur containing species: SO_4^{2-} and HSO_4^-. The consequence is the occurrence of only one transition time.

In the case of H_2SO_4 solution, the main concentrated specie is HSO_4^-, in the pH range measured during the chronopotentiometric analysis (pH 1.5 – 2.0), but small pH variations near the membrane surface can change the proportion of sulfate species. The speciation diagram presented in the Figure 4 indicates that the concentration of SO_4^{2-} achieves a steady value for pH higher than 4.0. Whereas the concentration of HSO_4^- continuously decrease until the pH achieves values around 9.0. As the pH is measured

in the bulk solution during the chronopotentiometric experiments (initial pH=1.85), the pH variations in the membrane-solution interface can be wider, affecting the ionic species concentration.

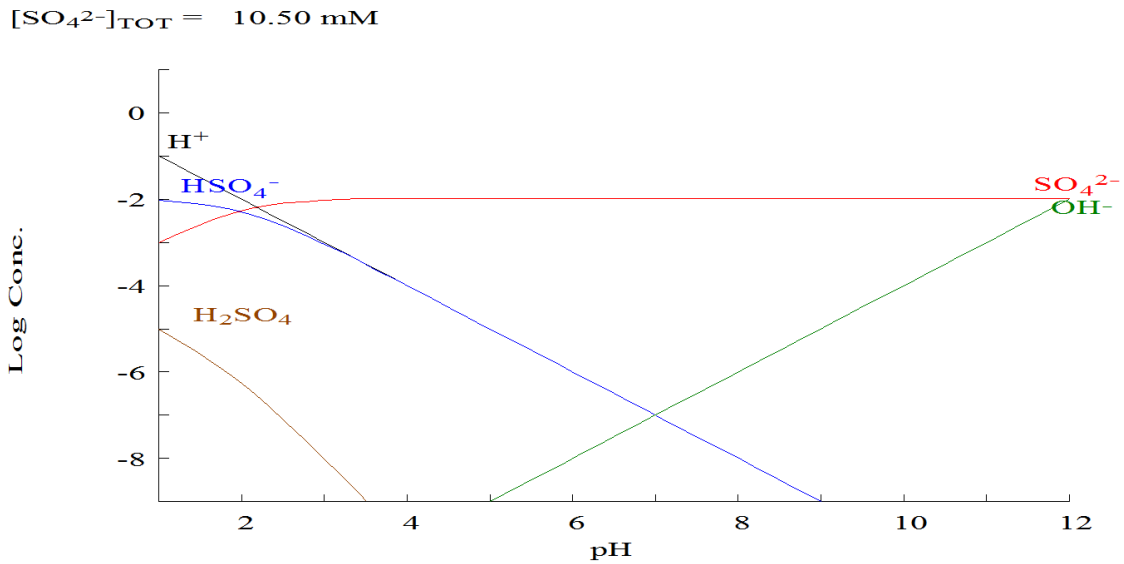

Figure 4. Speciation diagram for sulfuric acid solution 1.05□10^{-2} M.

Many authors investigated the transport of acids through anionic membranes [7,9,10,22–24] considering different solution concentrations, and suggesting how SO_4^{2-} and HSO_4^- are transported. Tugas et al [22] indicated that the positively charges of the anion exchange membrane are balanced by HSO_4^- ions, but, when an electric field is applied, only SO_4^{2-} ions are transported and the proton remains in the cathodic side. On the other hand, Jörrisen et al [24] indicated two mechanisms: one of them purposes that SO_4^{2-} enters in the membrane, combines with H^+, and the proton is prevented to return to the cathodic side; the other one suggest that the ion HSO_4^- enters in the membrane, and transfers one additional proton to the anodic side, but not avoid that the proton return to the cathodic side. Besides different theories, in recent studies, Le [25] verified using chronopotentiometric evaluation that, even if there are both SO_4^{2-} and HSO_4^- in equilibrium, only one inflexion point (transition time) was verified. Determining the transport number for sulfate ion, in a 0.1 M H_2SO_4 solution as 0.99 ± 0.04 [25]. In this case, the solution was tenfold more concentrated that the H_2SO_4 solution studied in the present paper.

According to the chronopotentiograms indicated in Figure 3, the two detected transition times could correspond to the transport of HSO_4^- and SO_4^{2-} ions. Probably the specie $[Ni(SO_4)_2]^{2-}$ was transported in the same transition time that HSO_4^-, since both presents similar concentrations in the nickel sulfate solution (Fig. 3a). For acid and the acidified solution, the main anionic species are HSO_4^- and SO_4^{2-}. As both anions have very similar concentration, only one transition time indicates that both are transported at the same time.

The effect of the acid can be observed also in the current-voltage curves (i-U_m) in Figure 5, obtained from the chronopotentiometric data. The i-U_m curves are in accordance with the concentration polarization and electroconvection theories since they display the three characteristic regions mentioned in the previous section. In all the comparative situations, it is possible to determine parameters as the limiting current density (i_{lim}), the ohmic resistance (R_{ohm}, $\Omega.cm^2$), the plateau length (ΔU_m, V), and the resistance in the region III (R_3, $\Omega.cm^2$). This data together with an additional information about the studied solutions are presented in Table 5, where the salts diffusion coefficients (D_{salt}) were obtained from equivalent conductivity data, λ, at infinite dilution using the Nernst–Einstein equation [26].

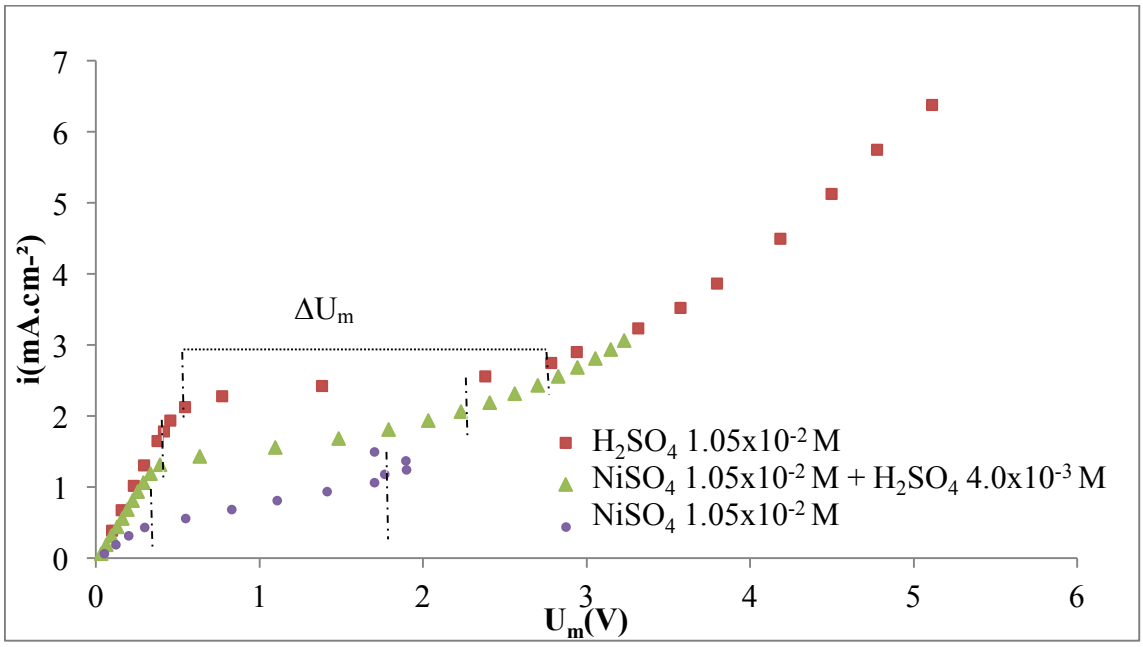

Figure 5. Current voltage curves of IONAC MA-3475 membrane in (a) nickel sulfate and sulfuric acid solutions.

Evaluating the *i*-U_m curves for nickel sulfate and the acidified solution, it must be inferred that increasing the initial acid concentration implies higher values of current density. According to the concentration polarization theory, the i_{lim} value can be expressed as a function of the initial electrolyte concentration (C_0) by means of the Peers' equation [27,28]

$$i_{lim} = \frac{zD_{salt}C_0F}{\delta\,(T_j - t_j)} \qquad \textbf{Equation 1}$$

where z is the valence of the ion, F is the Faraday's constant, D_{salt} is the salt diffusion coefficient, δ is the thickness of the diffusion boundary layer and T_j and t_j are the transport numbers of the ion j in the membrane and in the solution, respectively. Moreover, the salt diffusion coefficient also increases with the addition of acid, contributing to the rise in the limiting current density.

Table 5 - Limiting current, plateau length and resistance values for the anion exchange membrane IONAC MA-3475 in sulfate solutions.

Solution	$NiSO_4.6H_2O$	$NiSO_4.6H_2O+H_2SO_4$	H_2SO_4
Composition	$1.05\square10^{-2}$ M	$1.05\square10^{-2}$ M + $4.4\square10^{-3}$ M	$1.05\square10^{-2}$ M
$\mathbf{i_{lim}}$ **(mA.cm^{-2})**	0.46	1.19	2.25
$\mathbf{\Delta U_m}$ **(V)**	1.4	1.52	2.06
$\mathbf{R_{ohm}}$**(ohm.cm²)**	656.5	290.2	256
$\mathbf{R_3}$**(ohm.cm²)**	683.6	1063	804
$\mathbf{R_3/R_{ohm}}$	1.04	3.66	3.14
$\mathbf{D_{salt}}$ **($\square10^{-9}$ m².s^{-1})**	0.816	1.34[(a)]	2.60

(a) D_{salt} for bicomponent solutions: calculated considering the proportion of each component in the mixture.

When the H_2SO_4 solution is evaluated, although the sulfate concentration is equal to that for nickel sulfate solution, the limiting current density is higher. This increase in the current density value is in line with the salt diffusion coefficients. This confirms the fact that the main contributors for the anion transport during the quasi-ohmic region was not only the anions, but also the electric conductivity of the solutions, increased, in this

case, by the presence of H^+ [21], as previously discussed for the cronopotentiometric curves.

Previous studies [7,10] have already reported that anion-exchange membranes, in the presence of sorbed water, become proton conductors. The proton has specific properties and migrates by a mechanism which is fundamentally different from that observed for other ions due to its very high mobility. The proton transfer occurs through two mechanisms when AEMs are submitted to an electric field: the Grotthus mechanism and the classical co-ion leakage, when proton migrates like another sorbed cation [7]. A schematic representation of the ion transport throught the anion-exchange membrane is presented in Figure 6.

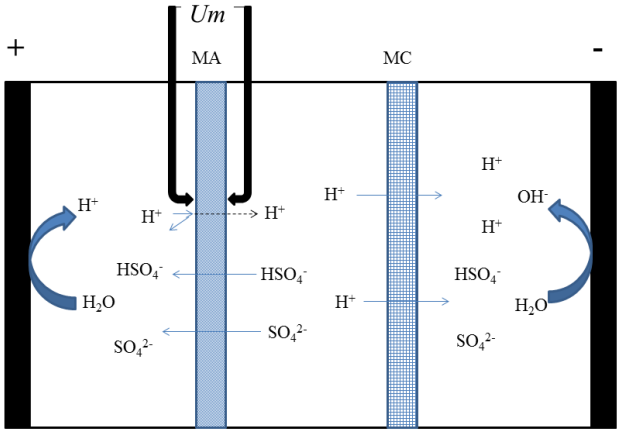

Figure 6. Schematic representation of ions transport through anion exchange membranes.

Comparing $NiSO_4$, $NiSO_4 + H_2SO_4$ and H_2SO_4 solutions, the transport of protons through the AEM could interfere in the transition time and the limiting current density for acid solutions. As reported by Lorrain et al [7], the rise in the concentration of acid in relation to the salt ([acid]/[acid+salt]) increases the transport number of the proton (proton leakage) through the AEM for a fixed current density. These effects are related to the low efficiency in electrodialysis and other electromembrane processes that aims to recover acids [7], once the membranes become more permeable to acids than to the salts. For nickel plating wastewater, acid can be added during the electrodialysis treatment in order to avoid the nickel precipitation on the membranes [29], therefore, electric current could be wasted in the transport of acid over the nickel.

The presence of sulfuric acid reflects directly in the ohmic resistance calculated for this group of sulfate solutions, as presented in Table 5. The R_{ohm} is an important

property that determines the contribution of the membrane resistance to the ion transport and the solution resistance in the adjacent diffusion layer in an electrodialytic process [4]. When H_2SO_4 was added, the electrical conductivity of the solutions increases, reducing the solution resistance [14] and the enrichment of the membrane phase with multivalent ions increases the electric conductivity of the membrane [30], as a consequence R_{ohm} decreases.

In the third region of the *i*-U_m curves, a new increment in the anions transport can be attributed to the other mechanisms of mass transfer, as the formation of water splitting products, or to convection related phenomena (gravitational or electrical), that bring the remaining ions in solution to the diffusion boundary layer [4,31]. Rubisntein et al [32] suggested that the heterogeneity of membranes surfaces can give a basis of an electroconvection mechanism which could produce characteristics of an overlimiting region. In this region III, is also possible determine the resistance (R_3), which is higher than R_{ohm} for the studied solutions, as observed in Table 5. Comparing the solutions, the lowest R_3 for $NiSO_4$ could be explained since in nickel solutions, the metallic ion in the interface membrane-solution can have a catalytic effect in hydrolysis reactions at overlimiting current densities [31].

The ratio of R_3 and R_{ohm} is related to the electroconvective effect and also hydrolysis reactions. According to Kang et al [31], the rise in the hydrolysis reactions reduces the membrane resistance in overlimiting current conditions. On the other hand, higher values for R_3/R_{ohm} (for solutions with H_2SO_4) can indicate a delay in the ions transport. The main contributor for the highest values of R_3 is the presence of H_2SO_4, which provides a high concentration of high mobility protons that can move through cationic and anionic membranes. The proton leakage is based on the exchange of H^+ ions between successive water molecules, either by a proton hopping mechanism (Grotthus mechanism) or by a succession of molecular rotations of the H_2O dipoles (Bjerrum fault mechanism)[7].

Between regions I and III of the *i*-U_m curves, in current densities near the i_{lim} value, the plateau length (ΔU_m) can be considered as the region where the main mechanism of ions transport changes from diffusion to convection [31] (electro-, gravitational convection or water splitting phenomena). Comparing the values presented in Table 5, the plateau length increases with the addition of sulfuric acid, and is bigger for H_2SO_4 solution. For this group of solutions the plateau length follows the same behavior of the solution electric conductivity and the salt diffusion coefficient.

Previous researches have already indicated a strong relation between the concentration and the plateau length [33]. According to the data showed in Table 4, the total concentration of anions in these solutions is higher for sulfuric acid solution. Additionally, the plateau length can be related to a measure of the power required to destroy the diffusion boundary layer. As the same membrane type was evaluated for both solutions, the difference in the solution concentration and the presence of H^+ can cause a delay in the phenomena expected in the third region, resulting in different plateau lengths and resistances.

The highest values for ΔU_m increase the potential for generating degradation products from water splitting, since that bigger electrical field has to be applied between the two sides of the membrane to achieve the transition to higher limiting currents. On the other hand, smaller ΔU_m values imply the occurrence of electroconvection preferably to the water dissociation. As presented by Martí-Calatayud et al [33], in $i>i_{lim}$, the ions transport is intensified and the displacement of the electroneutrality conditions facilitates the electroconvection and implies in a reduction of the plateau length. This ΔU_m value is directly related to the current efficiency and the electrodialysis costs of the wastewater treatment. Therefore, for nickel plating rinsewater, the acid addition is necessary in order to avoid nickel precipitation, even though pH adjustment will require more energy to destroy the diffusion boundary layer and take up the ions transport.

3.2. Effect of pH and co-ions properties

In order to evaluate the co-ion effect on the anion transport, the following solutions were studied: Na_2SO_4, $Na_2SO_4 + H_2SO_4$, $MgSO_4$ and $Na_2SO_4 + NiSO_4$. According to the chronopotentiograms shown in Figure 7, the anion transport behavior did not suffer major changes when sodium and nickel solutions with and without acid are compared (see Figure 3).

a)

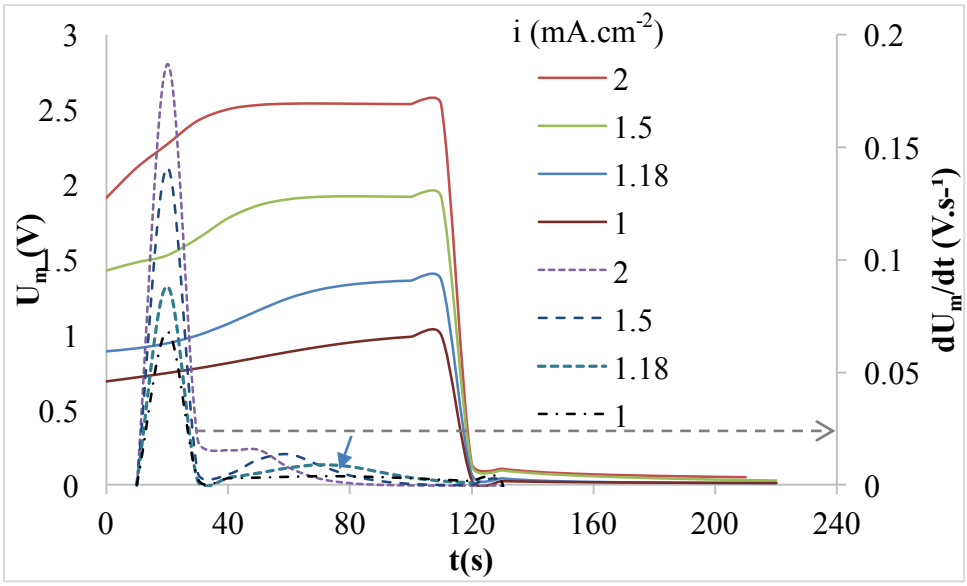
i (mA.cm-2)
2
1.5
1.18
1
2
1.5
1.18
1
Um (V)
dUm/dt (V.s-1)
t(s)
0
40
80
120
160
200
240
0
0.5
1
1.5
2
2.5
3
0
0.05
0.1
0.15
0.2

b)

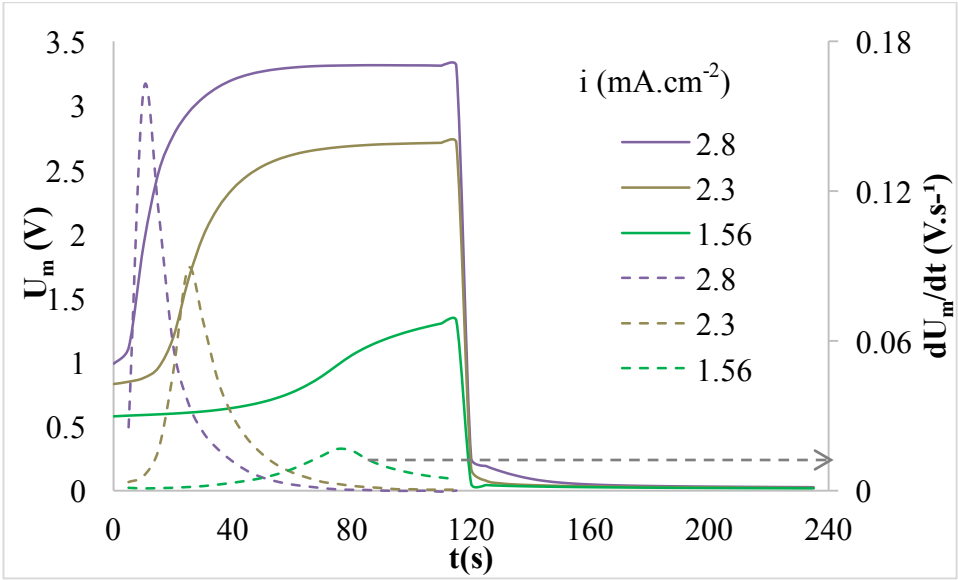
i (mA.cm-2)
2.8
2.3
1.56
2.8
2.3
1.56
Um (V)
dUm/dt (V.s-1)
t(s)
0
40
80
120
160
200
240
0
0.5
1
1.5
2
2.5
3
3.5
0
0.06
0.12
0.18

c)

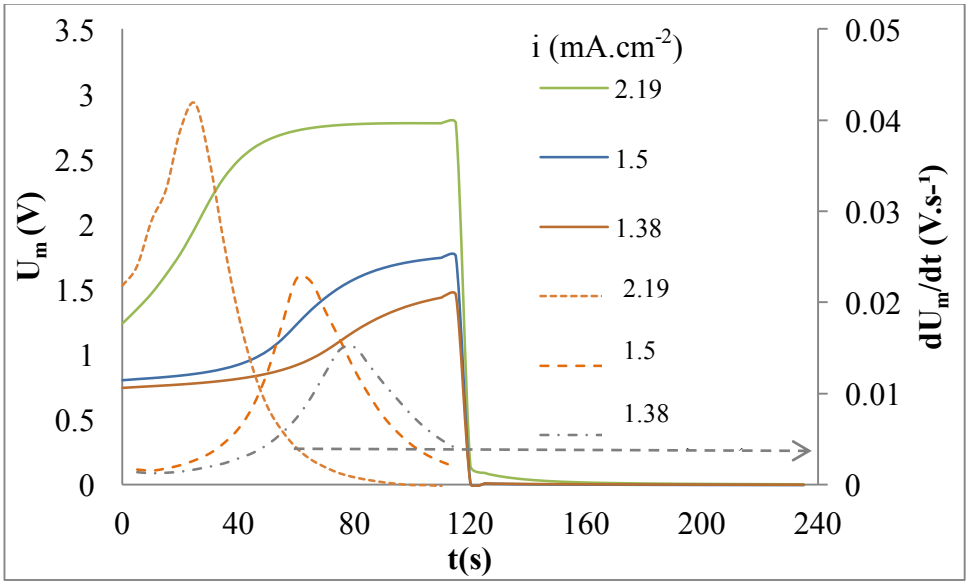
i (mA.cm-2)
2.19
1.5
1.38
2.19
1.5
1.38
Um (V)
dUm/dt (V.s-1)
t(s)
0
40
80
120
160
200
240
0
0.5
1
1.5
2
2.5
3
3.5
0
0.01
0.02
0.03
0.04
0.05

d)

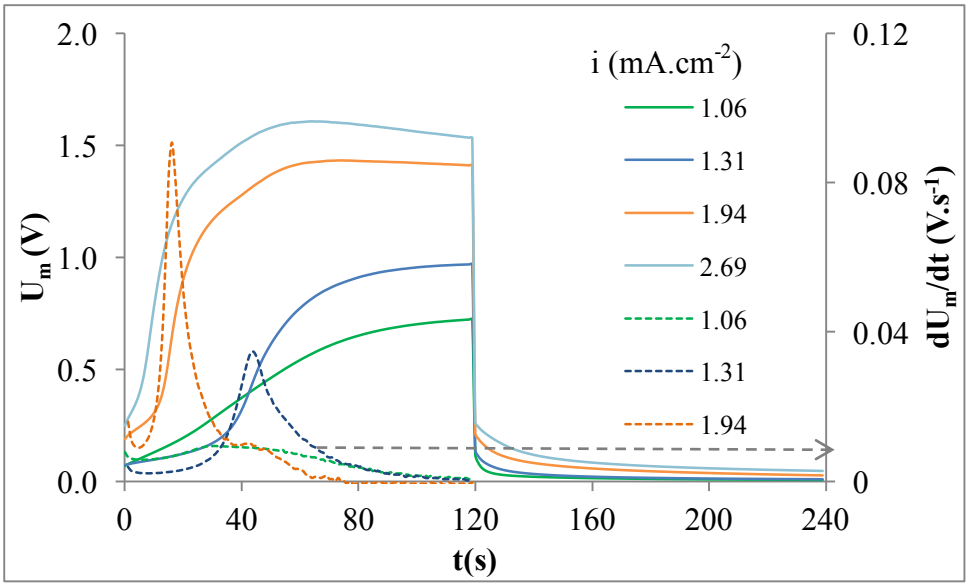

Figure 7. Chronopotentiometric curves obtained for the anion exchange membrane Ionac MA 3475 in (a) Na_2SO_4 1.05□10^{-2} M, (b) Na_2SO_4 1.05□10^{-2} M +H_2SO_4 1.1□10^{-3}M, (c) $MgSO_4$ 1.94□10^{-2} M and (d) Na_2SO_4 1.05□10^{-2} M +$NiSO_4$ 1.1 □10^{-3} M solutions. (Solid line: U_m (V); dashed line: dU_m/dt (V.s^{-1}).

Although the occurrence of two transition times was also detected for Na_2SO_4 (Figure 7 (a)), the negatively charged species change in this solution. As indicated in Table 6, the concentration of the main negatively charged species is: SO_4^{2-}> $Na_2SO_4^-$ > HSO_4^-. The equivalent charge (Q_{eq}) for these anions can be calculated considering the concentration of each specie (C_j) and its valence (z_i) [18]. Comparing the values of each ion, SO_4^{2-} is the main contributor in the transport of charges, followed by $NaSO_4^-$ ($Q_{eq}SO_4^{2-}$ =1.12□10^{-2} > $Q_{eq}NaSO_4^-$ =1.0□10^{-3}). When SO_4^{2-} ions are depleted from the solution/membrane interface the main charge carrier changes from SO_4^{2-} to $NaSO_4^-$ ions.

The addition of H_2SO_4 changes the anion concentration, and the concentration of HSO_4^- becomes equal to that of SO_4^{2-} as observed in Table 6. The equivalent charges in the acidified solution indicate that SO_4^{2-} and HSO_4^- ($Q_{eq}SO_4^{2-}$ =1.91□10^{-2} > $Q_{eq}HSO_4^-$ = 5.62□10^{-3}) contribute to the charge transport 30 times more than $NaSO_4^-$ ($Q_{eq}NaSO_4^-$ =5.0□10^{-4}). Hence, their transition times can be overlapped, as shown in Figure 7 (b).

Table 6 - Concentration (mol/L) of the species present in equilibrium as a function of the initial solution concentration and pH.

Solution Concentration	Na_2SO_4 1.05×10^{-2} M	$Na_2SO_4+H_2SO_4$ 1.05×10^{-2} M $+1\times10^{-3}$ M	$MgSO_4$ 1.94×10^{-2} M	$Na_2SO_4+NiSO_4$ 1.05×10^{-2} M+ 1.02×10^{-3} M
pH	8.2	1.9	6.7	7.2
$[Na^+]$	2.0×10^{-2}	2.09×10^{-2}	-	2.0×10^{-2}
$[Mg^{2+}]$	-	-	7.21×10^{-3}	
$[Ni^{2+}]$				1.26×10^{-4}
$[MgOH^+]$	-	-	2.0×10^{-7}	
$[NiOH^+]$				6.31×10^{-7}
$[H^+]$	6.31×10^{-9}	1.15×10^{-2}	2.0×10^{-7}	6.31×10^{-8}
$[OH^-]$	1.53×10^{-6}	-	4.68×10^{-8}	1.48×10^{-7}
$[NaSO_4^-]$	1.00×10^{-3}	5.01×10^{-4}	-	1.00×10^{-3}
$[Ni(SO_4)_2^{2-}]$				1.35×10^{-7}
$[SO_4^{2-}]$	9.55×10^{-3}	5.62×10^{-3}	7.21×10^{-3}	1.0×10^{-2}
$[HSO_4^-]$	5.81×10^{-9}	5.62×10^{-3}	2.0×10^{-7}	6.31×10^{-8}

The chronopotentiometric curves obtained for magnesium sulfate, present a behavior comparable to the previously seen in the acidified solutions, where only one transition time was detected. This fact may be explained in terms of the data presented in Table 6, where sulfate ion appears as the only predominant species in solution since its concentration is considerably higher.

For the bicomponent Na-Ni solution, although a more varied occurrence of ionic species, the main anionic charges are SO_4^{2-} and $NaSO_4^-$. The concentration of these species in the initial pH conditions is very similar to that in the Na_2SO_4 solution. In addition, the shape observed for the chronopotentiometric curves for Na_2SO_4 and bicomponent Na-Ni solution is similar, since the main component is Na_2SO_4, indicating the occurrence of a second transition time from 1.81 $mA.cm^{-2}$ onwards.

The transition times and respective current density are presented in Table 7. Comparing the chronopotentiograms in Figure 3 (a) $NiSO_4$ and Figure 7 (a) Na_2SO_4 and (d) bicomponent Na-Ni solution, the first transition time (τ) increased in the order: $Na_2SO_4 < Na_2SO_4 + NiSO_4 < NiSO_4$ for current densities equal to 1.0, 1.06 and

0.69 mA.cm^{-2}, respectively. This sequence suggests that, not only the sulfate concentration, but also the co-ion affects the counterion transport. The second transition time was detected in 1.3, 1.18 and 1.8 mA.cm^{-2} respectively, for $NiSO_4$, Na_2SO_4 and $Na_2SO_4 + NiSO_4$ that corresponds to the increase in the second most concentrated anionic specie for each solution (Table 4 and Table 6).

Table 7 – Transition times and respective current densities obtained in the chronopotentiograms of the solutions.

Solution	Na_2SO_4	$NiSO_4$	$Na_2SO_4 + NiSO_4$
Concentration	1.05□10^{-2} M	1.05□10^{-2} M	1.05 □10^{-2} M+1.02 □10^{-3} M
i_1 (mA.cm^{-2})	1.0	0.69	1.06
τ_1(s)	20	75	40
i_2 (mA.cm^{-2})	1.18	1.3	1.8
τ_2(s)	80	50	55

The current-voltage curves obtained for this second group of solutions are presented in the Figure 8.

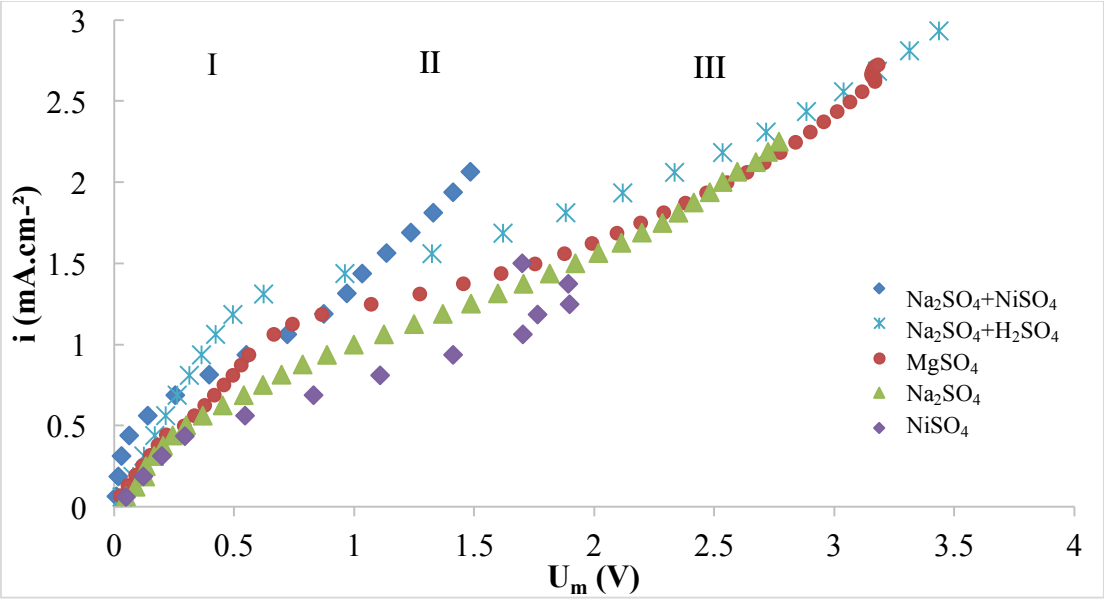

Figure 8. Current voltage curves of IONAC MA-3475 membrane in different sulfate solutions: $NiSO_4$ 1.05□10^{-2} M, Na_2SO_4 1.05□10^{-2} M, $MgSO_4$ 1.94□10^{-2} M, Na_2SO_4 1.05□10^{-2} M + $NiSO_4$ 1.1□10^{-3} M. and Na_2SO_4 1.5□10^{-2}M+H_2SO_4 1□10^{-3} M.

The most relevant data obtained from these i-U_m curves shown in Figure 8 are presented in Table 8. Comparing all studied solutions, the limiting current density is affected by the initial concentration and, as occurred for nickel sulfate, solutions containing acid presented higher i_{lim} values.

Table 8 - Limiting current, plateau length and resistance values for the anion exchange membrane IONAC MA-3475 in sulfate solutions.

Solution	Na_2SO_4	Na_2SO_4+H_2SO_4	$MgSO_4$	Na_2SO_4+$NiSO_4$
$\mathbf{i_{lim}}$ **(mA.cm^{-2})**	0.55	1.21	1.10	0.47
$\mathbf{\Delta U_m}$ **(V)**	1.94	2.08	1.52	0.91
$\mathbf{R_{ohm}}$**(ohm.cm²)**	520.4	410.6	661.9	95.8
$\mathbf{R_3}$**(ohm.cm²)**	972.3	1224.4	1097.5	753.8
$\mathbf{R_3/R_{ohm}}$	1.87	2.98	1.66	7.87
$\mathbf{D_{cation}}$ **(x 10^{-9} m².s^{-1})**	1.33	1.33[(a)]	0.706	1.33[(a)]
$\mathbf{D_{salt}}$ **(x 10^{-9} m².s^{-1})**	1.23	1.35[(b)]	0.849	1.19[(b)]

[(a)] D_{cation} considered the most concentrated cation in the solution

[(b)] D_{salt} for bicomponent solutions: calculated considering the proportion of each component in the mixture.

The effect of the counterion concentration is strongly present in the i-U_m curve for $MgSO_4$. This solution contains the highest concentration of sulfate anions, which reflects the proportional effect of the solution concentration on the i_{lim}. For the others nickel and sodium and also, the bicomponent Na-Ni solutions, the limiting current density values are close to 0.5 mA.cm^{-2}. The slight difference between i_{lim} for Na_2SO_4 and Na_2SO_4 + $NiSO_4$ solution suggest that the addition of nickel sulfate, though increase the solution concentration, can affect the transport mechanisms, reducing the i_{lim} value. This fact can be related to the salt diffusion coefficient – calculated for the mixed solution – also indicates a reduction after adding $NiSO_4$.

In the first region of the *i-U_m* curves the concentration gradients generated at the depleting side of the membrane are not limiting for the ion transfer through the membrane and the electrical resistance of the membrane-solution system (R_{ohm}) can be calculated from the inverse of the slope of this region. As indicated in Table 5 and Table 8, the ohmic resistance increases in the order: Na_2SO_4+$NiSO_4$ < Na_2SO_4< <$NiSO_4$ <$MgSO_4$, inversely to the values of the salt diffusion coefficients.

For the solutions containing sodium sulfate, according to Table 8, Na^+ presents the highest ion diffusion coefficient, conferring to Na_2SO_4 salt diffusion coefficient higher than the other salts. Thus the flux of ions from the bulk solution to the diffusion boundary layer is facilitated. Additionally, the highest ohmic resistance ($MgSO_4$ solution) matches with the smallest equivalent cationic charge (Q_{eq}^+) in the evaluated solutions. Furthermore, the hydrated ionic radius for the co-ions obeys the same behavior (Na^+=3.58 Å, Ni^{2+}=4.04 Å and Mg^{2+}=4.28 Å [34]). Considering that anion exchange membranes present non-ideal permselectivity and allows the co-ion leakage, the lowest availability of charges could raise the electrical resistance in the diffusion layer. Additionally, big hydrated radius hampers the ions transport through the ionic channels inside the membrane.

From the evaluation of the R_3/R_{ohm} ratio it is observed that this relation was in ascending order for Ni^{2+}, Mg^{2+} and Na^{2+} co-ions, achieving the highest value for the mixed Na-Ni solution. As discussed previously higher values for R_3/R_{ohm} can indicate a delay in the ion transport.

Comparing monocomponent solutions, the plateau length presents the same behavior that R_3/R_{ohm}. As the same membrane type was evaluated for both solutions, the difference in the solutions concentration can cause a delay in the phenomena expected in the third region, resulting in different plateau lengths.

According to the parameters presented in Table 5 and Table 8 the ascending order for R_3/R_{ohm}: Ni < Mg < Na match to the equivalent anionic charge (Q_{eq}^-) and the diffusion coefficients of the co-ions and their salts. The highest diffusion coefficients allow more ions to achieve the membrane from the bulk solution. This fact can delay the ion depletion in the diffusion boundary layer and, consequently, the occurrence of electroconvection reactions, since more anionic charges are in the membrane neighborhood to be transported.

Based on a similar evaluation of co-ions transport performed by Chamoulaud and Bélanger [14], the hydrated ionic radii and the charge density of each co-ion were considered. The Ni^{2+} and Mg^{2+} ions carry two positive charges and their hydrated ionic radii are 4.04 and 4.28 Å. Thus, they have a higher charge density than Na^+ (one positive charge and 3.58 Å). The values of charge density are 0.495, 0.467 and 0.279 for Ni^{2+}, Mg^{2+} and Na^+, consequently, the electrostatic interaction between the membrane and the co-ions is stronger with Ni^{2+} and Mg^{2+} than with Na^+, and allows for more facile transport of the Ni^{2+} co-ions across the anion exchange membrane [14]. With a stronger

electrostatic interaction and a lower charge concentration, the values of the plateau length tend to be lower for nickel than to the other ions.

The mixed solution sodium-nickel was studied in order to evaluate the possible synergic behavior of two co-ions. The reduction in the ohmic resistance and in plateau length when compared with Na_2SO_4 solution reveals that the addition of nickel could affect the ion transport mechanisms. Precipitation of nickel on the membranes was not observed, however, the presence of nickel indicated that additional ionic species can affect the formation and the collapse of the limiting diffusion layer, altering the energetic behavior in an electrodialytic system in the treatment of nickel plating rinsewater.

CONCLUSION

The study about different sulfate solutions and also mixed solutions and the influence of the co-ions on the anions transport was evaluated. The observed effects are interesting because when an electrodialysis treatment system is operated for nickel plating rinsewater, the effluent is a multicomponent solution whose pH and concentration are constantly changing. During the treatment, the system can vary from underlimiting to overlimiting current density, favoring or hampering the transport of ions, improving the efficiency or increasing operational costs.

The comparison of solutions with different compositions and concentration of anions indicated that the main effect on the limiting current density is the initial solution concentration, followed by the presence of acid. The transport of protons through the anionic membrane and their high mobility and conductivity are responsible for the highest values of i_{lim}. Solutions where two transition times were detected with the increase in the applied current, indicate that other anionic species in lower concentration were also transported, like HSO_4^- and anionic complexes as $[Ni(SO_4)_2]^{2-}$.

Electric resistances were reduced and the plateau length was increased by the presence of protons. For salts solutions (without acid) the highest diffusion coefficients gave the lowest ohmic resistances and co-ion hydrated radii were associated with the observed values. Higher i_{lim} could improve the transport of interesting ions, but also can represent a high cost and low efficiency. Thus, the knowledge about the wastewater composition and the transport phenomena through the membranes will determine the suitable parameters to obtain the efficiency in the application of electromembrane treatment processes.

Acknowledgements

This study was financially supported by Erasmus Brazilian Windows Puls (EBW+), CAPES, CNPq, BNDES, FINEP, SCIT and FAPERGS.

References

[1] T. Benvenuti, M.A.S. Rodrigues, A.M. Bernardes, J. Zoppas-Ferreira, Electrodialysis Treatment of Nickel Wastewater, in: A.M. Bernardes, M.A.S. Rodrigues, J. Zoppas-Ferreira (Eds.), Electrodialysis Water Reuse Nov. Approaches, Elsevier, 2014: p. 144. doi:10.1007/978-3-642-40249-4.

[2] K.-E. Bouhidel, M. Rumeau, Ion-exchange membrane fouling by boric acid in the electrodialysis of nickel electroplating rinsing waters: generalization of our results, Desalination. 167 (2004) 301–310. doi:10.1016/j.desal.2004.06.139.

[3] M.C. Martí-Calatayud, M. García-Gabaldón, V. Pérez-Herranz, Effect of the equilibria of multivalent metal sulfates on the transport through cation-exchange membranes at different current regimes, J. Memb. Sci. 443 (2013) 181–192. doi:10.1016/j.memsci.2013.04.058.

[4] M.C. Martí-Calatayud, M. García-Gabaldón, V. Pérez-Herranz, E. Ortega, Determination of transport properties of Ni(II) through a Nafion cation-exchange membrane in chromic acid solutions, J. Memb. Sci. 379 (2011) 449–458. doi:http://dx.doi.org/10.1016/j.memsci.2011.06.014.

[5] A.T. Cherif, C. Gavach, Electro-transport of sulphuric acid by electro-electrodialysis, J. Electroanal. Chem. Interfacial Electrochem. 265 (1989) 143–157. doi:10.1016/0022-0728(89)80185-8.

[6] S. Koter, M. Kultys, B. Gilewicz-Łukasik, I. Koter, Modeling the transport of sulfuric acid and its sulfates (MgSO4, ZnSO4, Na2SO4) through an anion-exchange membrane, Desalination. 342 (2014) 75–84. doi:10.1016/j.desal.2013.10.025.

[7] Y. Lorrain, G. Pourcelly, C. Gavach, Influence of cations on the proton leakage through anion-exchange membranes, J. Memb. Sci. 110 (1996) 181–190. doi:10.1016/0376-7388(95)00246-4.

[8] B.J. Robbins, R.W. Field, S.T. Kolaczkowski, A.D. Lockett, Rationalisation of the relationship between proton leakage and water flux through anion exchange

membranes, J. Memb. Sci. 118 (1996) 101–110. doi:10.1016/0376-7388(96)00095-6.

[9] S. Koter, M. Kultys, Electric transport of sulfuric acid through anion-exchange membranes in aqueous solutions, J. Memb. Sci. 318 (2008) 467–476. doi:10.1016/j.memsci.2008.03.010.

[10] Y. Lorrain, G. Pourcelly, C. Gavach, Transport mechanism of sulfuric acid through an anion exchange membrane, Desalination. 109 (1997) 231–239. doi:10.1016/S0011-9164(97)00069-6.

[11] P. Ray, V.K. Shahi, T. V. Pathak, G. Ramachandraiah, Transport phenomenon as a function of counter and co-ions in solution: Chronopotentiometric behavior of anion exchange membrane in different aqueous electrolyte solutions, J. Memb. Sci. 160 (1999) 243–254. doi:10.1016/S0376-7388(99)00088-5.

[12] G. Ramachandraiah, P. Ray, Electroassisted Transport Phenomenon of Strong and Weak Electrolytes across Ion-Exchange Membranes: Chronopotentiometric Study on Deactivation of Anion Exchange Membranes by Higher Homologous Monocarboxylates, J. Phys. Chem. B. 101 (1997) 7892–7900. doi:10.1021/jp9701698.

[13] L. Marder, V. Perez-Herranz, Electrodialysis Control Parameters, in: A.M. Bernardes, M.A.S. Rodrigues, J. Zoppas-Ferreira (Eds.), Electrodialysis Water Reuse Nov. Approaches., Springer, 2014: p. 144.

[14] G. Chamoulaud, D. Bélanger, Modification of ion-exchange membrane used for separation of protons and metallic cations and characterization of the membrane by current–voltage curves, J. Colloid Interface Sci. 281 (2005) 179–187. doi:10.1016/j.jcis.2004.08.081.

[15] K. Sollner, Ion exchange membranes, Ann. New York Acad. Sci. (n.d.) 177–203.

[16] L. Marder, E.M. Ortega Navarro, V. Pérez-Herranz, A.M. Bernardes, J.Z. Ferreira, Evaluation of transition metals transport properties through a cation-exchange membrane by chronopotentiometry, J. Memb. Sci. 284 (2006) 267–275. doi:10.1016/j.memsci.2006.07.039.

[17] M.C. Martí-Calatayud, D.C. Buzzi, M. García-Gabaldón, A.M. Bernardes, J.A.S. Tenório, V. Pérez-Herranz, Ion transport through homogeneous and heterogeneous ion-exchange membranes in single salt and multicomponent electrolyte solutions, J. Memb. Sci. 466 (2014) 45–57. doi:10.1016/j.memsci.2014.04.033.

[18] M. García-Gabaldón, V. Pérez-Herranz, E. Ortega, Evaluation of two ion-exchange membranes for the transport of tin in the presence of hydrochloric acid, J. Memb. Sci. 371 (2011) 65–74. doi:10.1016/j.memsci.2011.01.015.

[19] M. Wang, X. Wang, Y. Jia, X. Liu, An attempt for improving electrodialytic transport properties of a heterogeneous anion exchange membrane, Desalination. 351 (2014) 163–170. doi:10.1016/j.desal.2014.07.039.

[20] P. Długołęcki, B. Anet, S.J. Metz, K. Nijmeijer, M. Wessling, Transport limitations in ion exchange membranes at low salt concentrations, J. Memb. Sci. 346 (2010) 163–171. doi:10.1016/j.memsci.2009.09.033.

[21] J.-H. Choi, H.-J. Lee, S.-H. Moon, Effects of Electrolytes on the Transport Phenomena in a Cation-Exchange Membrane., J. Colloid Interface Sci. 238 (2001) 188–195. doi:10.1006/jcis.2001.7510.

[22] I. Tugas, J.M. Lambert, J. Maillols, J.L. Bribes, G. Pourcelly, C. Gavach, Identification of the ionic species in anion exchange membranes equilibrated with sulphuric acid solutions by means of Raman spectroscopy and radiotracers, J. Memb. Sci. 78 (1993) 25–33. doi:10.1016/0376-7388(93)85244-Q.

[23] G. Pourcelly, I. Tugas, C. Gavach, Electrotransport of HCl in anion exchange membranes for the recovery of acids. Part II. Kinetics of ion transfer at the membrane-solution interface, J. Memb. Sci. 85 (1993) 195–204. doi:10.1016/0376-7388(93)85168-V.

[24] J. Jörissen, S.M. Breiter, C. Funk, Ion transport in anion exchange membranes in presence of multivalent anions like sulfate or phosphate, J. Memb. Sci. 213 (2003) 247–261. doi:10.1016/S0376-7388(02)00532-X.

[25] X.T. Le, Contribution to the study of properties of Selemion AMV anion exchange membranes in acidic media, Electrochim. Acta. 108 (2013) 232–240. doi:10.1016/j.electacta.2013.07.011.

[26] D. Lide, CRC handbook of chemistry and physics, Http://Www.Hbcpnetbase.Com. (2005).

[27] P. Sistat, G. Pourcelly, Chronopotentiometric response of an ion-exchange membrane in the underlimiting current-range. Transport phenomena within the diffusion layers, J. Memb. Sci. 123 (1997) 121–131. doi:10.1016/S0376-7388(96)00210-4.

[28] J.J. Krol, M. Wessling, H. Strathmann, Chronopotentiometry and overlimiting ion transport through monopolar ion exchange membranes, J. Memb. Sci. 162

(1999) 155–164. doi:10.1016/S0376-7388(99)00134-9.

[29] T. Benvenuti, M.A. Siqueira Rodrigues, A.M. Bernardes, J. Zoppas-Ferreira, Closing the loop in the electroplating industry by electrodialysis, J. Clean. Prod. (2016). doi:10.1016/j.jclepro.2016.05.139.

[30] N. Pismenskaya, E. Laktionov, V. Nikonenko, A. El Attar, B. Auclair, G. Pourcelly, Dependence of composition of anion-exchange membranes and their electrical conductivity on concentration of sodium salts of carbonic and phosphoric acids, J. Memb. Sci. 181 (2001) 185–197. doi:10.1016/S0376-7388(00)00529-9.

[31] M.-S. Kang, Y.-J. Choi, H.-J. Lee, S.-H. Moon, Effects of inorganic substances on water splitting in ion-exchange membranes: I. Electrochemical characteristics of ion-exchange membranes coated with iron hydroxide/oxide and silica sol, J. Colloid Interface Sci. 273 (2004) 523–532. doi:10.1016/j.jcis.2004.01.050.

[32] I. Rubinstein, B. Zaltzman, Electro-convective versus electroosmotic instability in concentration polarization, Adv. Colloid Interface Sci. 134 (2007) 190–200. doi:10.1016/j.cis.2007.04.013.

[33] M.C. Martí-Calatayud, M. García-Gabaldón, V. Pérez-Herranz, Study of the effects of the applied current regime and the concentration of chromic acid on the transport of Ni2+ ions through Nafion 117 membranes, J. Memb. Sci. 392 (2012) 137–149. doi:10.1016/j.memsci.2011.12.012.

[34] E.R. Nightingale, Phenomenological Theory of Ion Solvation. Effective Radii of Hydrated Ions, J. Phys. Chem. 63 (1959) 1381–1387. doi:10.1021/j150579a011.